

REPORT DOCUMENTATION PAGE			Form Approved OMB NO. 0704-0188		
<p>The public reporting burden for this collection of information is estimated to average 1 hour per response, including the time for reviewing instructions, searching existing data sources, gathering and maintaining the data needed, and completing and reviewing the collection of information. Send comments regarding this burden estimate or any other aspect of this collection of information, including suggestions for reducing this burden, to Washington Headquarters Services, Directorate for Information Operations and Reports, 1215 Jefferson Davis Highway, Suite 1204, Arlington VA, 22202-4302. Respondents should be aware that notwithstanding any other provision of law, no person shall be subject to any penalty for failing to comply with a collection of information if it does not display a currently valid OMB control number.</p> <p>PLEASE DO NOT RETURN YOUR FORM TO THE ABOVE ADDRESS.</p>					
1. REPORT DATE (DD-MM-YYYY) 30-11-2014		2. REPORT TYPE Final Report		3. DATES COVERED (From - To) 1-Aug-2013 - 30-Apr-2014	
4. TITLE AND SUBTITLE Final Report: Improve the Performance of Integrated Diode Laser Beam Combining Through Grating Regrowth			5a. CONTRACT NUMBER W911NF-13-1-0254		
			5b. GRANT NUMBER		
			5c. PROGRAM ELEMENT NUMBER 611102		
6. AUTHORS Lin Zhu			5d. PROJECT NUMBER		
			5e. TASK NUMBER		
			5f. WORK UNIT NUMBER		
7. PERFORMING ORGANIZATION NAMES AND ADDRESSES Clemson University 300 Brackett Hall Clemson, SC 29634 -5702			8. PERFORMING ORGANIZATION REPORT NUMBER		
9. SPONSORING/MONITORING AGENCY NAME(S) AND ADDRESS (ES) U.S. Army Research Office P.O. Box 12211 Research Triangle Park, NC 27709-2211			10. SPONSOR/MONITOR'S ACRONYM(S) ARO		
			11. SPONSOR/MONITOR'S REPORT NUMBER(S) 63908-EL-II.1		
12. DISTRIBUTION AVAILABILITY STATEMENT Approved for Public Release; Distribution Unlimited					
13. SUPPLEMENTARY NOTES The views, opinions and/or findings contained in this report are those of the author(s) and should not be construed as an official Department of the Army position, policy or decision, unless so designated by other documentation.					
14. ABSTRACT This project aims to improve the output power and coherence of monolithically combined broad-area diode lasers through grating regrowth. We have recently demonstrated coherent beam combining in a new, completely integrated approach to edge-emitting semiconductor lasers. Modal control has been achieved through angled transverse Bragg grating approach that creates 100 micron wide lasers with a single mode, and two such lasers have been combined (through two dimensional Bragg diffraction) in a "V" pattern to create a diffraction-limited beam. The coherence has been verified via double slit interference pattern created at the "V" side where the two separate					
15. SUBJECT TERMS diode lasers; beam combining; modal control					
16. SECURITY CLASSIFICATION OF:			17. LIMITATION OF ABSTRACT UU	15. NUMBER OF PAGES	19a. NAME OF RESPONSIBLE PERSON Lin Zhu
a. REPORT UU	b. ABSTRACT UU	c. THIS PAGE UU			19b. TELEPHONE NUMBER 864-656-4381

Report Title

Final Report: Improve the Performance of Integrated Diode Laser Beam Combining Through Grating Regrowth

ABSTRACT

This project aims to improve the output power and coherence of monolithically combined broad-area diode lasers through grating regrowth. We have recently demonstrated coherent beam combining in a new, completely integrated approach to edge-emitting semiconductor lasers. Modal control has been achieved through angled transverse Bragg grating approach that creates 100 micron wide lasers with a single mode, and two such lasers have been combined (through two dimensional Bragg diffraction) in a "V" pattern to create a diffraction-limited beam. The coherence has been verified via double slit interference pattern created at the "V" side where the two separate lasers emit. The output power of the demonstrated lasers is currently limited by the deeply etched (1.2 um) surface gratings. We propose to create the grating near the active region so that the grating depth could be reduced to about 50nm. After the grating is etched, the P waveguide/cladding/contact layers will be re-grown on top of the grating. This regrowth process will greatly reduce the scattering loss and surface defects induced by the grating and result in uniform current injection, which will ultimately improve the performance of coherently combined broad area lasers.

Enter List of papers submitted or published that acknowledge ARO support from the start of the project to the date of this printing. List the papers, including journal references, in the following categories:

(a) Papers published in peer-reviewed journals (N/A for none)

Received

Paper

TOTAL:

Number of Papers published in peer-reviewed journals:

(b) Papers published in non-peer-reviewed journals (N/A for none)

Received

Paper

TOTAL:

Number of Papers published in non peer-reviewed journals:

(c) Presentations

Number of Presentations: 0.00

Non Peer-Reviewed Conference Proceeding publications (other than abstracts):

Received Paper

TOTAL:

Number of Non Peer-Reviewed Conference Proceeding publications (other than abstracts):

Peer-Reviewed Conference Proceeding publications (other than abstracts):

Received Paper

TOTAL:

Number of Peer-Reviewed Conference Proceeding publications (other than abstracts):

(d) Manuscripts

Received Paper

TOTAL:

Number of Manuscripts:

Books

Received Book

TOTAL:

Received Book Chapter

TOTAL:

Patents Submitted

Patents Awarded

Awards

Yunsong Zhao (graduate student) the Hitachi High Technologies America Electron Microscopy Annual Fellowship

Graduate Students

<u>NAME</u>	<u>PERCENT SUPPORTED</u>	Discipline
Yunsong Zhao	0.50	
FTE Equivalent:	0.50	
Total Number:	1	

Names of Post Doctorates

<u>NAME</u>	<u>PERCENT SUPPORTED</u>
FTE Equivalent:	
Total Number:	

Names of Faculty Supported

<u>NAME</u>	<u>PERCENT SUPPORTED</u>	National Academy Member
Lin Zhu	0.20	
FTE Equivalent:	0.20	
Total Number:	1	

Names of Under Graduate students supported

<u>NAME</u>	<u>PERCENT SUPPORTED</u>	Discipline
Justin Vo	0.50	
FTE Equivalent:	0.50	
Total Number:	1	

Student Metrics

This section only applies to graduating undergraduates supported by this agreement in this reporting period

The number of undergraduates funded by this agreement who graduated during this period: 1.00

The number of undergraduates funded by this agreement who graduated during this period with a degree in science, mathematics, engineering, or technology fields:..... 1.00

The number of undergraduates funded by your agreement who graduated during this period and will continue to pursue a graduate or Ph.D. degree in science, mathematics, engineering, or technology fields:..... 1.00

Number of graduating undergraduates who achieved a 3.5 GPA to 4.0 (4.0 max scale):..... 0.00

Number of graduating undergraduates funded by a DoD funded Center of Excellence grant for Education, Research and Engineering:..... 0.00

The number of undergraduates funded by your agreement who graduated during this period and intend to work for the Department of Defense 1.00

The number of undergraduates funded by your agreement who graduated during this period and will receive scholarships or fellowships for further studies in science, mathematics, engineering or technology fields:..... 0.00

Names of Personnel receiving masters degrees

<u>NAME</u>
Total Number:

Names of personnel receiving PHDs

<u>NAME</u>
Total Number:

Names of other research staff

<u>NAME</u>	<u>PERCENT SUPPORTED</u>
FTE Equivalent:	
Total Number:	

Sub Contractors (DD882)

Inventions (DD882)

Scientific Progress

Please see the attached report.

Technology Transfer

Final report: Improve the performance of integrated diode laser beam combining through grating regrowth

This project aims to improve the output power and coherence of monolithically combined broad-area diode lasers through grating regrowth. We have recently demonstrated coherent beam combining in a new, completely integrated approach to edge-emitting semiconductor lasers. Modal control has been achieved through angled transverse Bragg grating approach that creates 100 micron wide lasers with a single mode, and two such lasers have been combined (through two dimensional Bragg diffraction) in a "V" pattern to create a diffraction-limited beam. The coherence has been verified via double slit interference pattern created at the "V" side where the two separate lasers emit. The output power of the demonstrated lasers is currently limited by the deeply etched (1.2 μm) surface gratings. We propose to create the grating near the active region so that the grating depth could be reduced to about 50nm. After the grating is etched, the P waveguide/cladding/contact layers will be re-grown on top of the grating. This regrowth process will greatly reduce the scattering loss and surface defects induced by the grating and result in uniform current injection, which will ultimately improve the performance of coherently combined broad area lasers.

1. Previous Designs

Figure 1 shows a schematic of the coherently combined angled-grating laser. Our laser device is fabricated in an InP-based multiple quantum well (MQW) epitaxy wafer. The combined laser cavity consists of two sets of angled-gratings that tilt to opposite directions with the same angle. The overlap area of the two gratings defines a two dimensional coupling region. The phase locking of two emitters is obtained by the wave coupling through Bragg diffraction in this overlap region. The resonance wavelength is chosen to be around 1550nm. To effectively couple two emitters and reduce modal loss in gratings, the tilt angle θ is set to be 10° . Accordingly, the period of gratings can be calculated to be 1.368 μm . The dimensions of a single emitter are 1.3mm \times 130 μm (L \times W). The etch depth of 1.0 μm is chosen to obtain a grating coupling coefficient around 0.1/ μm . Light is confined by gratings transversely and by total internal reflection vertically.

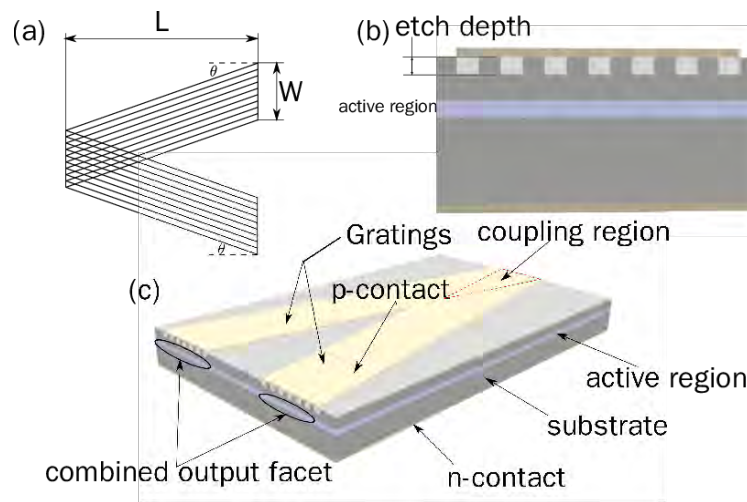


Figure 1 Schematic of a coherently combined angled-grating laser. (a) L and W are the length and width of a single emitter, respectively. θ is the tilt angle of the grating. (b) The cross section structure. (c) Planar geometry of the

combined angled-grating laser. Two coherently combined emitters (two legs in the coupled structure) constructively interfere in the far field.

2. Limitations of surface gratings

As shown in Fig. 1, we use a surface grating approach to realize modal control and beam combining. Compared to the buried grating approach, this method is relatively simple and does not require epi-wafer regrowth. However, in order to obtain sufficient grating coupling coefficients and minimize the metal contact absorption losses, the gratings depth usually needs to be larger than $1\mu\text{m}$. In our demonstration, the surface grating is obtained through reactive ion etching, which always leads to a certain level of surface roughness and defects and subsequently results in photon and carrier losses for the fabricated laser device. In addition, the laser needs to be planarized by BCB to prevent the metal contact from falling into the etched grating trenches. Since BCB is insulator, the resistance of the planarized grating is higher than the outside region. Thus, the current distribution is not uniform when we inject the current through the top metal contact. Figure 2 shows the simulation result of the current distribution of the planarized laser. It is clear that the current density is higher around two edges and lower in the middle region. This non-uniform current distribution could excite high order Bragg modes and reduce the coherence of the combined beam.

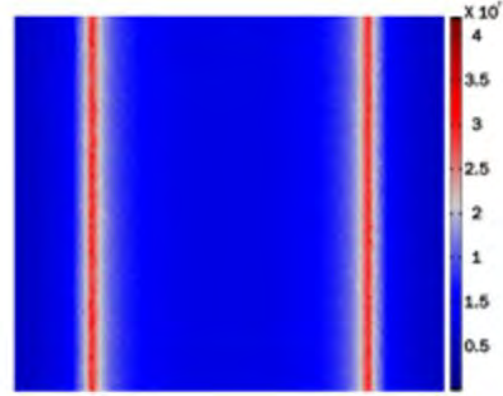


Figure 2 Nonuniform current distribution of the planarized laser (top view).

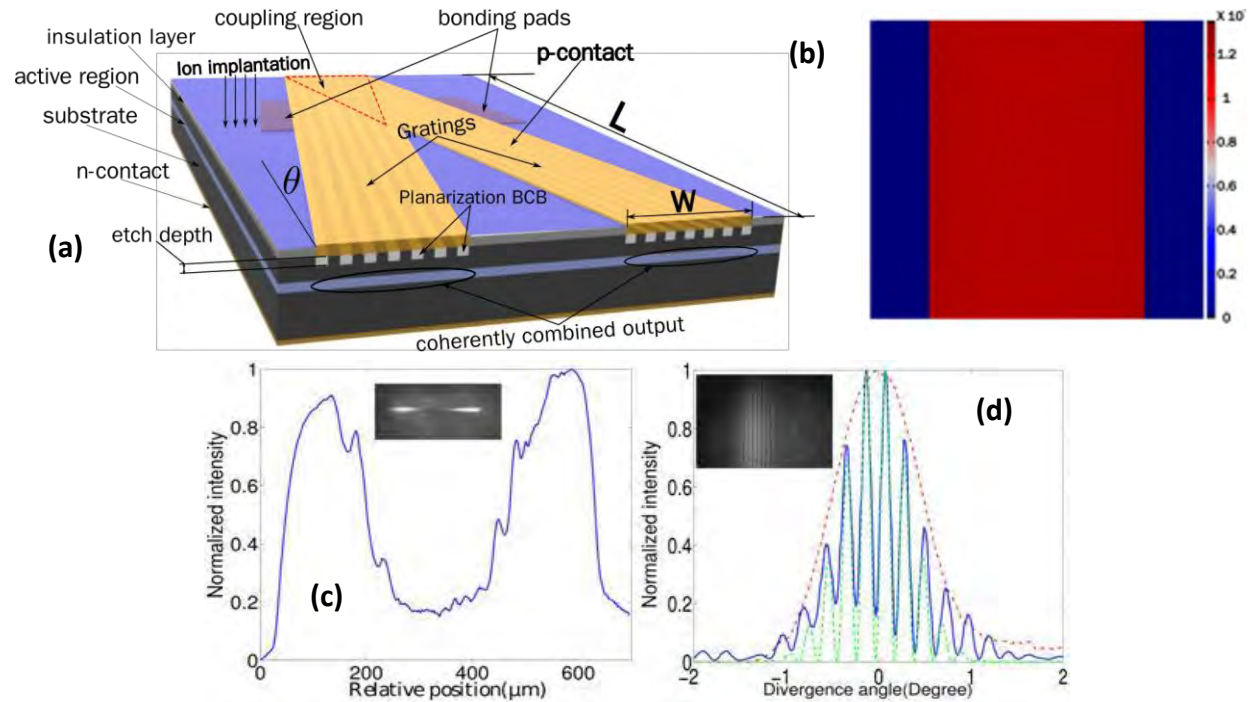


Figure 3 (a) Ion-implanted laser device. The blue area on top represents the ion-implanted region. (b) Current distribution of ion-implanted laser. The distribution becomes uniform after increasing the resistance outside the grating area through ion implantation. (c) Near field of the coupled laser. The inset is the camera image. (d) Far field profiles: the blue solid line is the measured far field of the coupled laser, the green dashed line is the calculated far

field and the red dash-dot line represents the measured far field of a single angled-grating broad-area laser. We obtain a good agreement between the measured and calculated far field. The inset is the camera image.

To verify our analysis, we increase the resistance of the materials outside of the grating region through ion implantation to obtain a much more uniform current distribution, as shown in Fig. 3 (a) and (b). Figure 3 (c) and (d) show the near field and far field measurement results of our laser, respectively. In the near field, the total width of the emitting aperture is about 160 μ m and the distance between the two apertures is about 426 μ m. There is about 10% difference in the intensities of the two beams. These values will be used in the theoretical far-field calculation. Compared with the samples without implantation, the near-field profile of the ion implanted lasers has sharper edges of the emitting apertures and larger distinction ratio between the emitting area and dummy area due to better current confinement. In the far field shown in Fig. 7(d), an overall single lobe envelope is obtained. Multiple fringes in the far field are due to the interference of two coherently combined emitters. The full width at half maximum (FWHM) is about 1.08°. The angular distance between fringes is about 0.207°. Compared with the previous far-field result without implantation, a much better contrast ratio of the interference fringes is obtained. The difference between peaks and valleys for our previous device is only about 0.2. In our current device, the difference is improved to be 0.9 in the normalized scale, which indicates better coherence of the two emitters. We also show the comparison between the measured far field (solid line) and the calculated result (dashed line). The angular distance between fringes in the calculated result is about 0.2040°. We obtain good agreement between the two results.

Our experimental results prove that the planarized surface grating indeed results in nonuniform current distribution and limits the laser performance. Ion implantation outside of the grating region could solve this problem and leads to better beam quality and coherence of the combined lasers. **However, the optical and electrical losses induced by the surface grating still limit the laser output power and efficiency.**

3. Buried grating design in GaAs

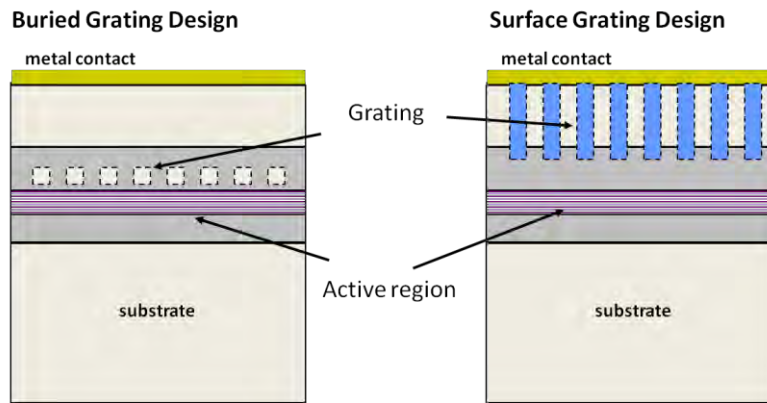


Figure 4 The proposed buried grating design vs surface grating design.

The buried grating approach is proposed to overcome the limitation of surface gratings and improve the combined laser performance, as shown in Fig. 4. Since the buried grating is much closer to the quantum well gain region, the grating confinement factor is much larger so that the grating depth could be reduced two orders of magnitude. This helps reduce the scattering losses of the fabricated laser devices. The shallow grating depth also implies that wet etching may be used to fabricate the grating, which will reduce the surface defects/ recombination centers. Furthermore, the cladding layer will be regrown on top of the grating, which also helps to

remove the surface defects. With the buried grating approach, the resistance of the grating region will not be higher than the outside region since no insulation is used. This means that we should not have the nonuniform current distribution problem.

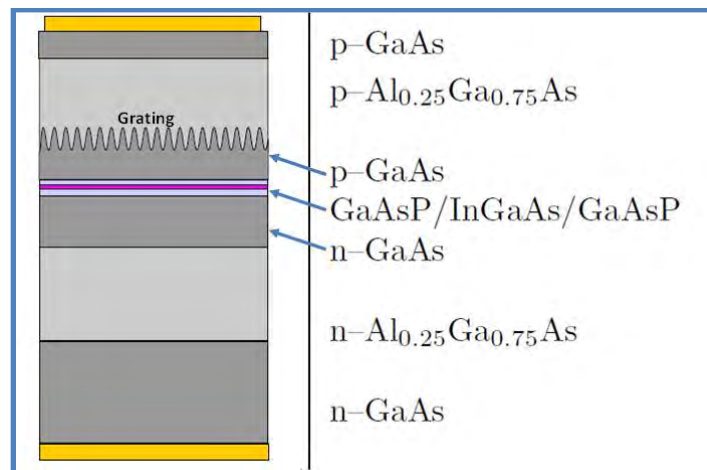


Figure 5 The buried grating design in GaAs

We will demonstrate the buried grating design for integrated broad area laser beam combining in AlGaAs-GaAs materials to obtain high power and efficiency. Our wafer design with the regrown grating is shown in Fig. 5. The AlGaAs/GaAs material system with InGaAs quantum wells is very well suitable for high power diode lasers due to its excellent optical and electrical properties. However, AlGaAs is not ideal for the grating regrowth process due to the potential possibility of Aluminum oxidization. We solve this problem by using GaAs as the waveguide layer and etch the grating in GaAs, as shown in Fig. 5. Compared to AlGaAs, the bandgap of GaAs is a little bit smaller. Thus, we shift the lasing wavelength longer to about 1060nm by modifying the Indium content in the InGaAs quantum well so that the carrier confinement is sufficient even with the GaAs waveguide layer. Two thin GaAsP layers shown in Fig. 5 are used for strain compensation.

Our experimental progresses are summarized in the following ppt slides.

Summary

- We have designed and fabricated three patterns: single alpha DFB lasers, two-coupled lasers and four-coupled lasers, each with three different etching depth of 25nm, 85nm and 140nm in the regrowth wafer
- Samples with 85nm etching depth were shipped back first and we have finished measurements on these devices. The other samples were returned later and we have finished the device fabrication and started the measurements on these devices but not finished yet
- Some samples were broken during shipping which contaminated the samples. This may produce roughness during regrowth and degrade the performance of the final devices.

Epitaxy wafer structure

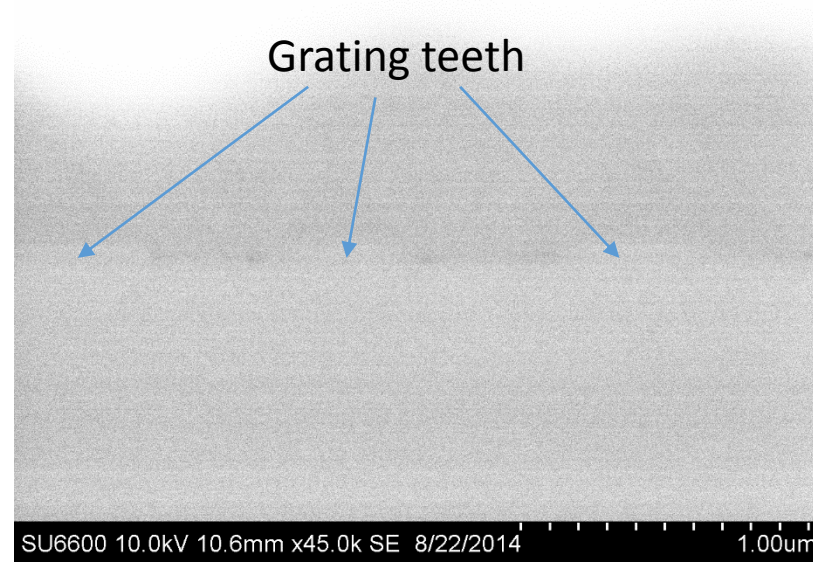
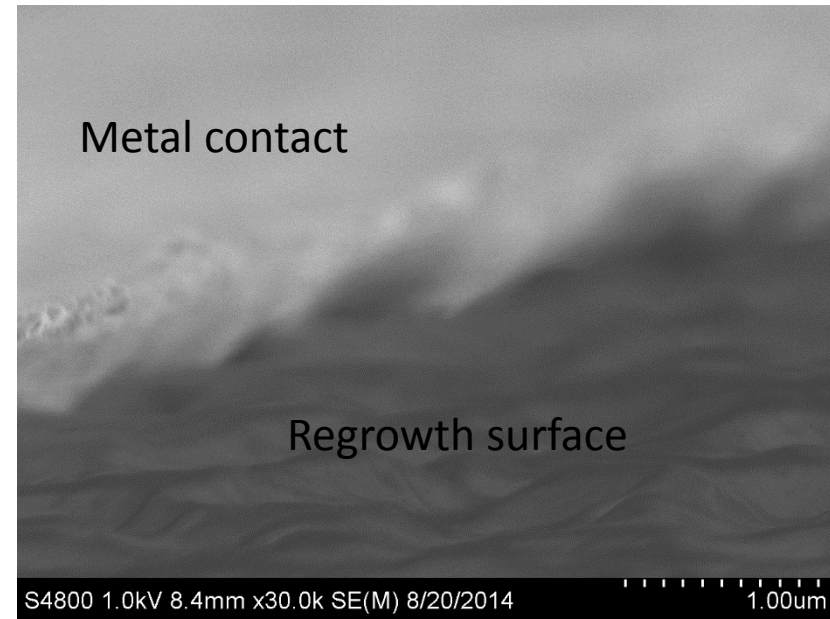
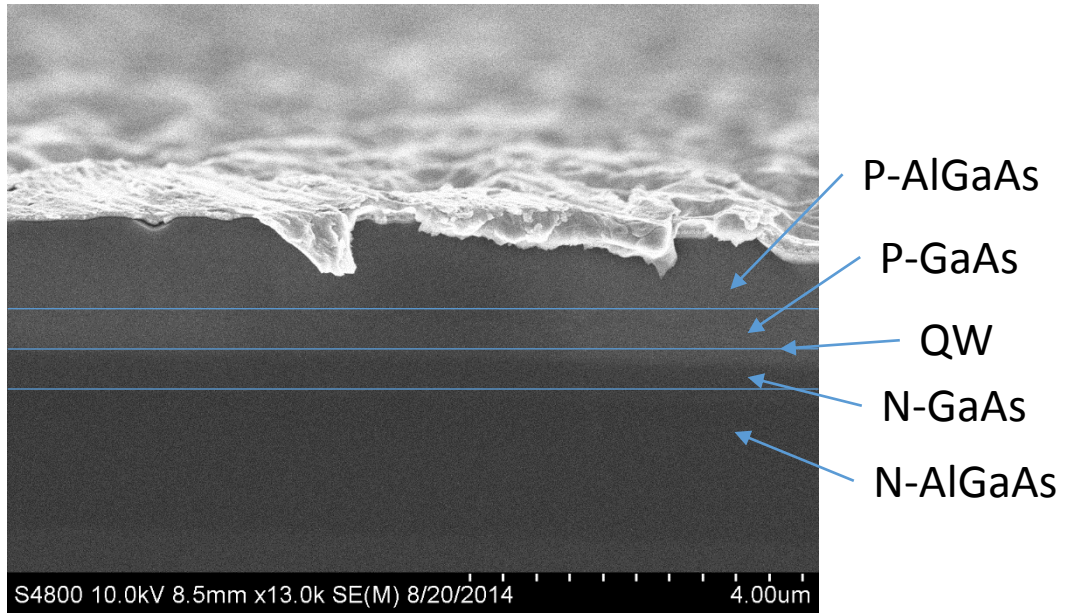
Layer	Description	Material	Thickness(nm)	Dopant	Doping Level	Doping Type
1	Substrate	GaAs	n/a	Si	2e18	N
2	Cladding	$\text{Al}_{0.25}\text{Ga}_{0.75}\text{As}$	1360	Si	2e18	N
3	Waveguide	GaAs	400	Si	1e17 ~ 1e18	N
4	Barrier	$\text{GaAs}_{0.9}\text{P}_{0.1}$	12	n/a	n/a	undoped
5	Quantum Well	$\text{In}_{0.28}\text{Ga}_{0.72}\text{As}$	8	n/a	n/a	undoped
6	Barrier	$\text{GaAs}_{0.9}\text{P}_{0.1}$	12	n/a	n/a	undoped
7	Waveguide	GaAs	400	C	1e17 ~1e18	P
8	Cladding	$\text{Al}_{0.25}\text{Ga}_{0.75}\text{As}$	940	C	2e18	P
9	Contact Layer	GaAs	50	C	2e19	P

- Gratings are etched in the P-type GaAs Waveguide layer(Layer 7) and then planarized by Layer 8 and 9 through the following regrowth process;
- PL measurement shows that the peak wavelength is around 1061nm.

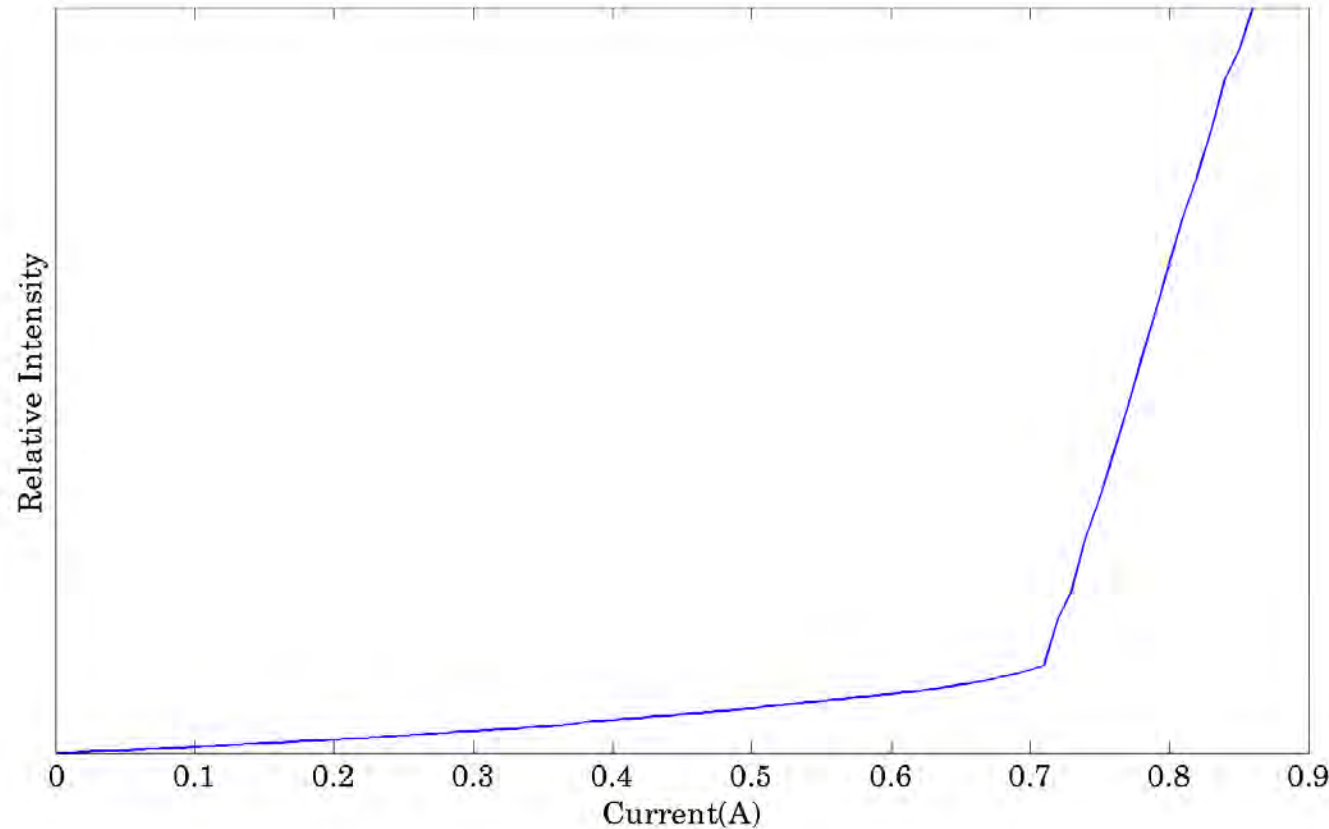
Fabrication process

- The epiwafer first starts with 100nm SiO₂ deposition which is used as the etching mask;
- Grating patterns are defined and written by Ebeam lithography, then transferred in SiO₂ by dry etching;
- Patterns are transferred in GaAs through wet etching in H₂SO₄:H₂O₂:H₂O solution;
- After removing SiO₂ in BOE, samples are shipped to foundry service for the regrowth process;
- When samples return, metal contacts are deposited. The devices are finalized by cleavage and packaging, and ready for measurement.

SEM pictures

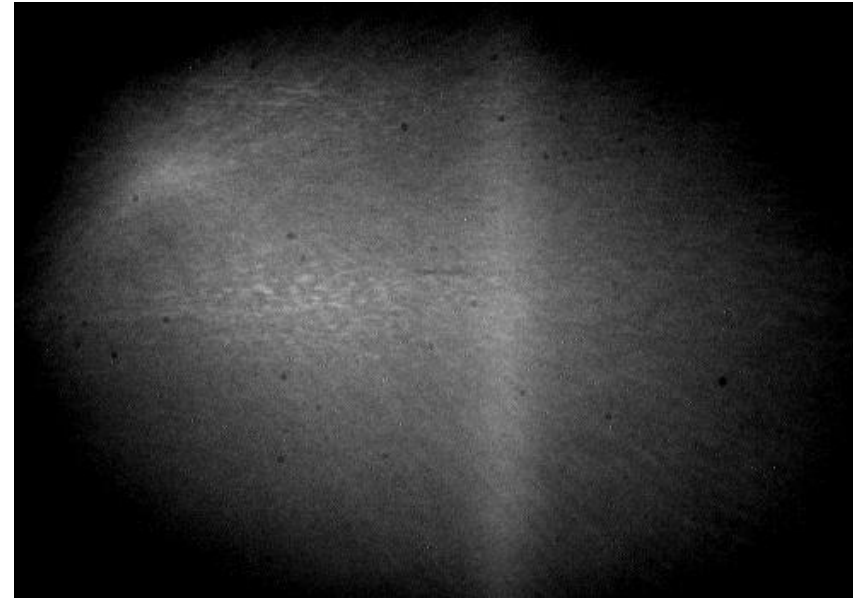
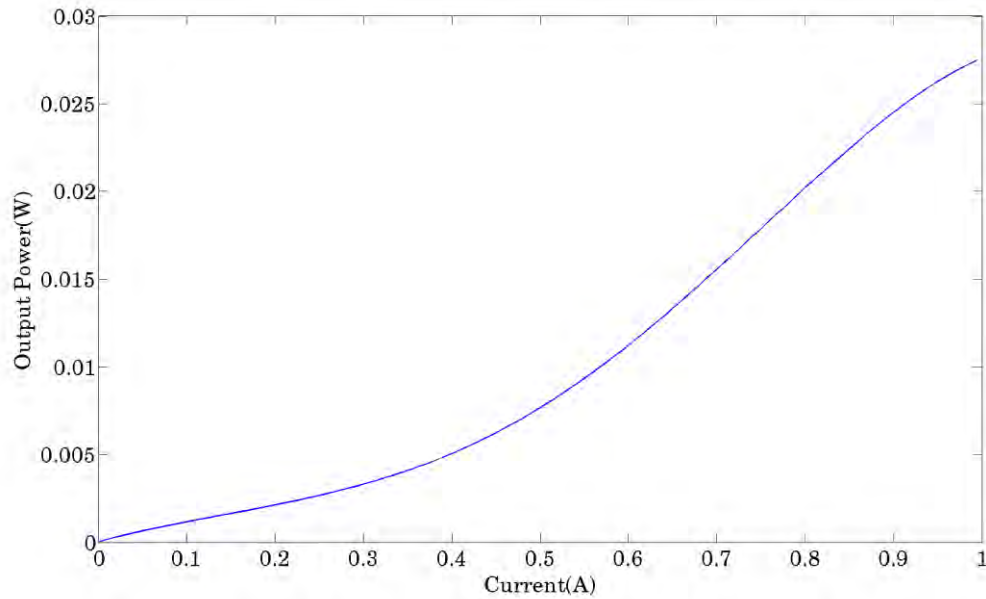


Broad-area laser in regrowth epi wafer



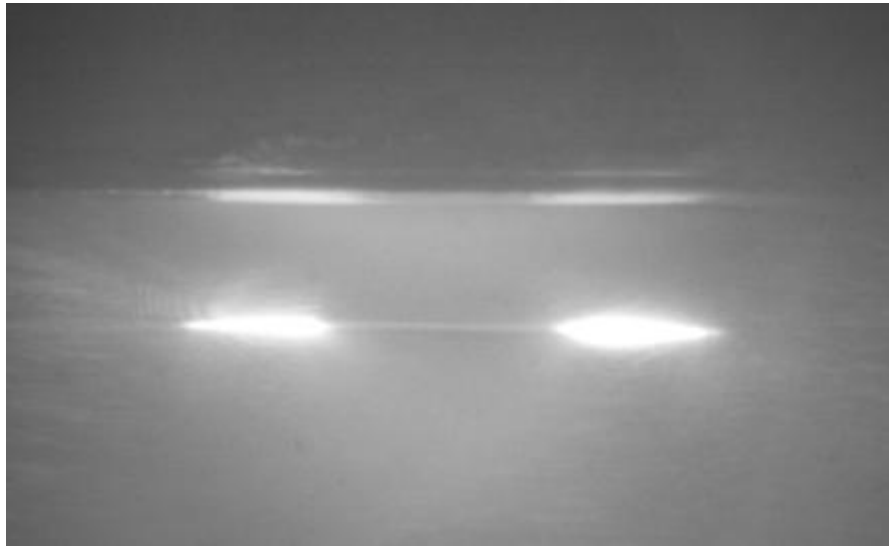
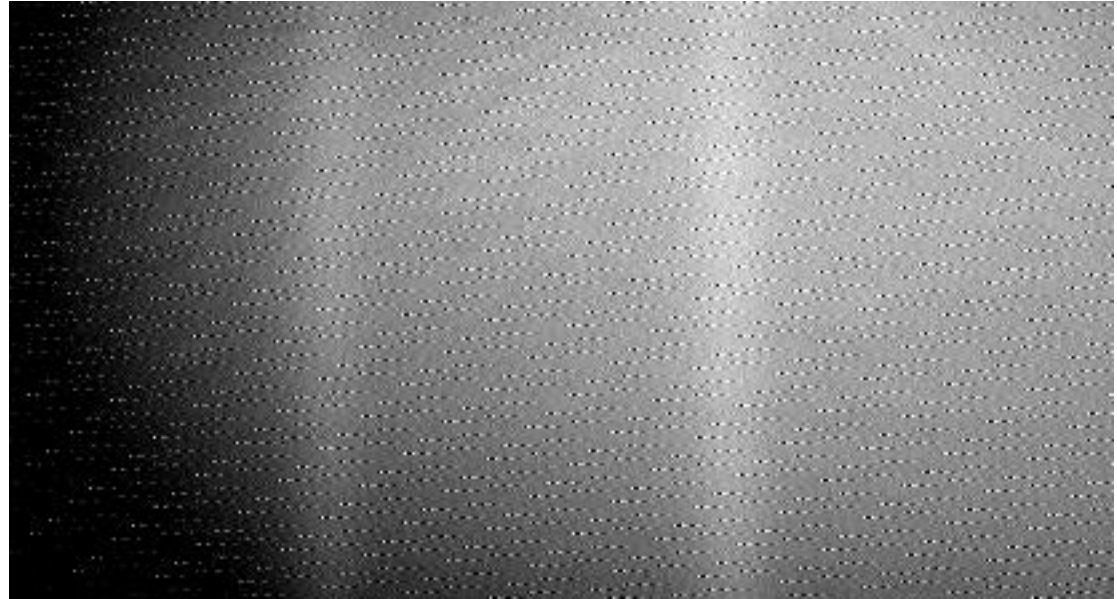
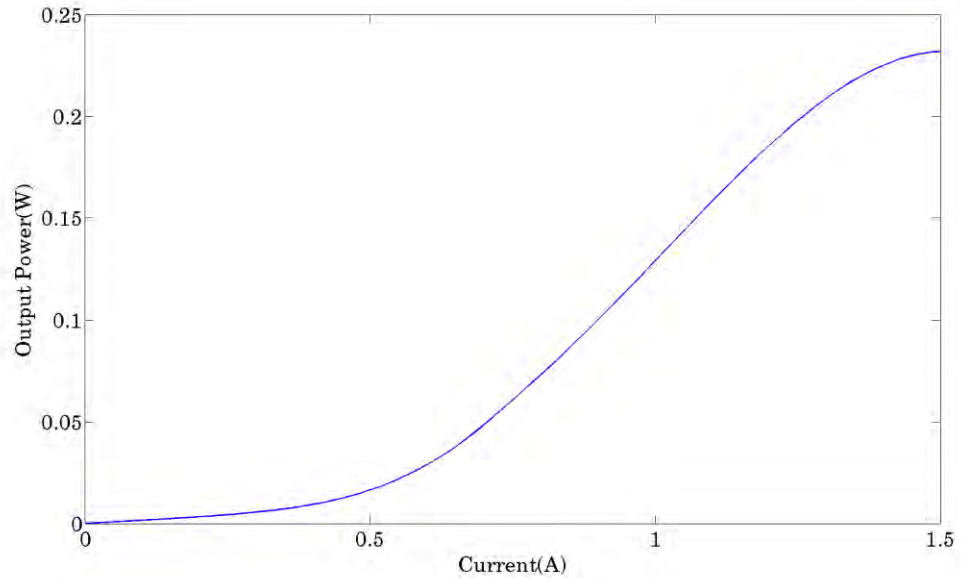
- L-I curve measured with pulse current source in room temperature;
- High threshold is due to the contamination.

Single α DFB laser with 85nm etch depth



- L-I curve is measured in low temperature (100K);
- Near field and far field pics were taken at the current of 1A;
- Far field remains stable and single lobe;
- No current leakage due to ion implantation as shown in near field.

Two coupled α DFB laser with 85nm etch depth



- L-I curve was measured in low temperature (100K);
- Near field and far field pics were taken at the current of 1.2A ;
- Far field shows double lobes, indicating that the two emitters are not combined. This may be due to the shallow etch in the coupling region. The 2D coupling region has shallower etch depth because of a slower wet etch rate compared to the 1D grating.